

**STRUCTURAL AND OPTICAL ANALYSIS OF
A LANDSAT TELESCOPE MIRROR**

by

Thomas E. Wolverton
John J. Brooks

Santa Barbara Research Center
Goleta, California

Contract No. NA-84-DSC-00125

*Presented at the 1987 MSC/NASTRAN World User's Conference
March 11 & 12, 1987
Los Angeles, California*

STRUCTURAL AND OPTICAL ANALYSIS OF A LANDSAT TELESCOPE MIRROR

by

Thomas E. Wolverton
John J. Brooks

Santa Barbara Research Center
Goleta, California

ABSTRACT

Finite element techniques were employed to determine distortions and subsequent image characteristics of the primary telescope mirror in a LANDSAT scanning spectral radiometer. Mirror deformations due to gravity and the presence of friction loads in kinematic mirror mounts were determined using the static analysis capabilities of MSC/NASTRAN. Displacement results were then postprocessed by PDA/PATRAN to create optical pseudo-spot diagrams indicating image degradation. These focal plane spot diagrams provide a convenient graphical method for quickly identifying critical load cases and predicting results of optical testing.

This work was performed under subcontract for the Earth Observation Satellite Company (EOSAT), and under prime contract for the U.S. Department of Commerce (LANDSAT) under contract number NA-84-DSC-00125.

INTRODUCTION

The NASA earth-remote-sensing research program employs the LANDSAT spacecraft to acquire earth resource data. Since 1978, the primary imaging sensor for the LANDSAT system has been the Thematic Mapper (TM), named for its ability to produce radiometrically and geometrically accurate maps of crops, forests, urban and rural areas, and to identify the signatures, or "themes" of plants, minerals, and other constituents of the environment [1].

The Thematic Mapper is a spectral radiometer that uses a scanning optical system to view a 185 kilometer wide swath on the surface of the earth while in a 9:30 A.M. polar orbit. Figure 1 illustrates the chief optical functions of the TM telescope. Within the optical system is a Ritchey-Chretien telescope consisting of a primary mirror and a secondary mirror. To insure optical image quality, the surface of the primary mirror must be kept within strict deformation tolerances. Seemingly small structural loads on the mirror can yield surface deformations sufficient enough to cause significant optical errors at the focal plane of the telescope.

Previous TM instruments have rigidly mounted the primary mirror to its telescope housing resulting in noticeable distortions in the mirror due to loads resulting from assembly. A proposed enhanced version of the TM (or ETM) to be employed by the Earth Observation Satellite Company (EOSAT), required an improved optical image; therefore, a need arose for a kinematic mounting system for the ETM primary mirror such that structural loads from the surrounding telescope housing are not imparted to the mirror. A mounting system was designed such that each rigid body motion of the mirror was constrained only once. Figure 2 is a simplified diagram of the ETM primary mirror mounting system. The mirror is mounted at three locations, 120 degrees apart. Each mount consists of a sleeve bearing contained within a ball joint, so that only the normal and tangential displacements are constrained while the radial displacement and all rotations are released. This type of mounting system, if truly frictionless would isolate the primary mirror from distorting structural loads.

Friction in the bearings, however, does contribute loading to the mirror. Though relatively low, there was some concern that resulting deformation due to friction in the mounting bearings could be significant enough to optically degrade the mirror surface. Structural analysis was therefore performed on the mirror.

DEFORMATION ANALYSIS OF THE PRIMARY MIRROR

The ETM primary mirror is constructed of a ultra-low expansion glass material (ULE), with a top and bottom face sheet and a lattice core structure, similar to a honeycomb composite. Using PDA/PATRAN [2], a finite element model was constructed of the mirror consisting of MSC/NASTRAN [3] QUAD4 plate elements for the webs and face sheets. Eight-noded HEXA elements were also used to model the tabs at the locations of the mounting bearings. Figure 3 shows the entire finite element model while Figure 4 shows the model with a portion removed so that the internal lattice structure can be seen.

The neutral surface of the optical face of the mirror was assumed to be spherical and was modeled with plate elements. However the optical surface of the mirror is actually hyperboloidal (slightly aspherical) and the displacements at the optical surface are desired, therefore dependent node points were placed on the hyperboloidal mirror surface and attached using massless rigid RBAR elements to the neutral surface elements (Figure 5). The displacements of these dependent nodes at the mirror surface are planned to be used as input data into an optical ray tracing program called CODE-V.

Loading conditions studied included in-plane and out-of-plane gravity loads and various combinations of radial and torsional loads at the mounting locations, representing loads produced by bearing friction. While the operating state of the mirror in orbit will not include gravity loads, they were considered since there will be extensive on-earth optical testing of the mirror prior to launch.

OPTICAL ASSESMENT OF FOCAL PLANE DEGRADATION

Displacement results of the mirror structure were postprocessed using PDA/PATRAN. Figure 6 is a typical deformed structure plot of the mirror in a 1-g gravity field normal to the focal plane with frictionless mount bearings. Simple deformed structure plots revealed distorted mirror shapes but did not give direct information about the optical impact of the deformed shape. While the displacement results could eventually be optically analyzed using a ray tracing program, it became apparent that a method was needed to quickly identify optically critical load cases.

An additional set of dependent nodes was placed at a point on the optical axis at a distance equal to twice the effective focal length of the Ritchey-Chretien mirror set. Each of these nodes was connected to an independent mirror

surface node with a massless RBAR element. These "ray bar" elements represent light rays converging to the focal plane. Figure 7 is an illustration of these "ray bar" elements extending from the mirror surface to the focal plane. By placing them at twice the focal length, the angle-doubling effect at the primary mirror surface is automatically included. Thus, as the surface of the mirror distorts under load, the surface nodes rotate, and the focal plane nodes spread to form a spot diagram, which is a display form familiar to optical engineers [4].

The displacement results of the endpoints of the "ray bar" elements were postprocessed using a FORTRAN program to convert displacement records into PATRAN phase-I commands (driven by a PATRAN session file) so that the displaced points could be plotted on a target. These resulting "pseudo-spot" diagrams provide an indication of how much the focal point degrades for a given load case. Figure 8 is a "pseudo-spot" diagram for the frictionless bearing, out-of-plane 1-g gravity case as shown in Figure 6. The target is the optical rms blur circle representing the distortion budget allocated to structural loads on the mirror. As long as 68% of the rays fall within this circle, the distortion budget has not been exceeded. The advantage of these pseudo-spot diagrams is that they can provide a quick, simple and inexpensive prediction of the optical ray trace results for each load case, providing immediate results without having to wait for complex ray tracing of each load condition.

It should be noted that there are some limitations to this technique. When examining the pseudo-spot diagram, consideration should be made to the fact that the "ray bar" elements do not represent equal increments of mirror surface area. One stray dot outside of the optical target could be significant if it represents a relatively large zone of optical surface. Another limitation of the pseudo-spot diagrams is that they do not give the "best focus" condition. The spot patterns are based on the original focal length and do not consider the possible improvement gained by refocusing the system.

CONCLUSIONS AND RECOMMENDATIONS

NASTRAN deformation analysis and pseudo-spot diagrams predict deformations to the primary mirror to be within the optical budget for the system. Figure 9 is a pseudo-spot diagram for a 1-g gravity load in the plane of the mirror. This is the orientation of the mirror during on-earth testing and shows considerable improvement from the out-of-plane gravity case as given in Figure 8. Many combinations of in-plane gravity and friction loads were considered with the worst case being the in-plane gravity combined

with full torsional and radial friction loads at all mounts as shown in Figure 10. Even the worst case complies with the optical budget and thereby indicates that the design goals for the kinematic mirror mounts have been met.

The post processing of finite element displacement results using the pseudo-spot diagram technique provides a useful mechanism for examining the optical response of deformed mirror surfaces. Optical analysis results for the primary mirror have yet to be obtained to verify the accuracy of this technique. Certain improvements could be made to enhance the spot diagram method, such as weighting the "ray bar" points based on the incremental mirror surface area they represent. Dots on the pseudo-spot diagram could have different symbol types, or sizes to correspond to their mirror surface areas. A technique is also now being considered to provide for refocusing at the focal plane. This may involve a different approach to post processing using a specially written plotting program instead of PDA/PATRAN.

REFERENCES

1. "Thematic Mapper, Design Through Flight Evaluation - Final Report", Santa Barbara Research Center, 1984
2. PDA/PATRAN *User's Guide, Release 1.5*, PDA Engineering, 1984
3. MSC/NASTRAN *Handbook For Linear Analysis, Version 64*, The MacNeal-Schwendler Corp., 1985
4. Smith, W. J., *Modern Optical Engineering*, McGraw-Hill, 1966

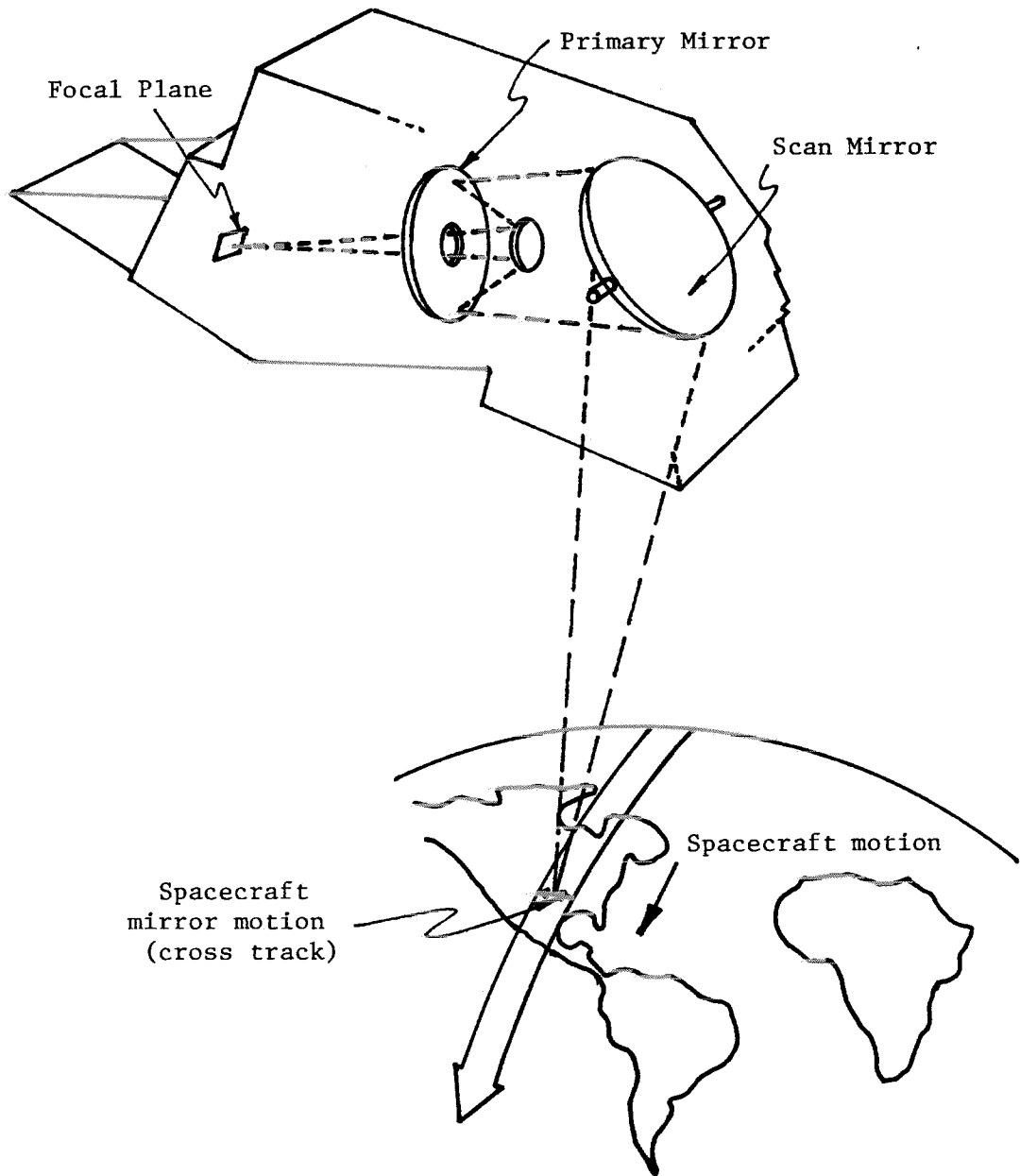


Figure 1. Thematic Mapper Ritchey-Chretien Telescope

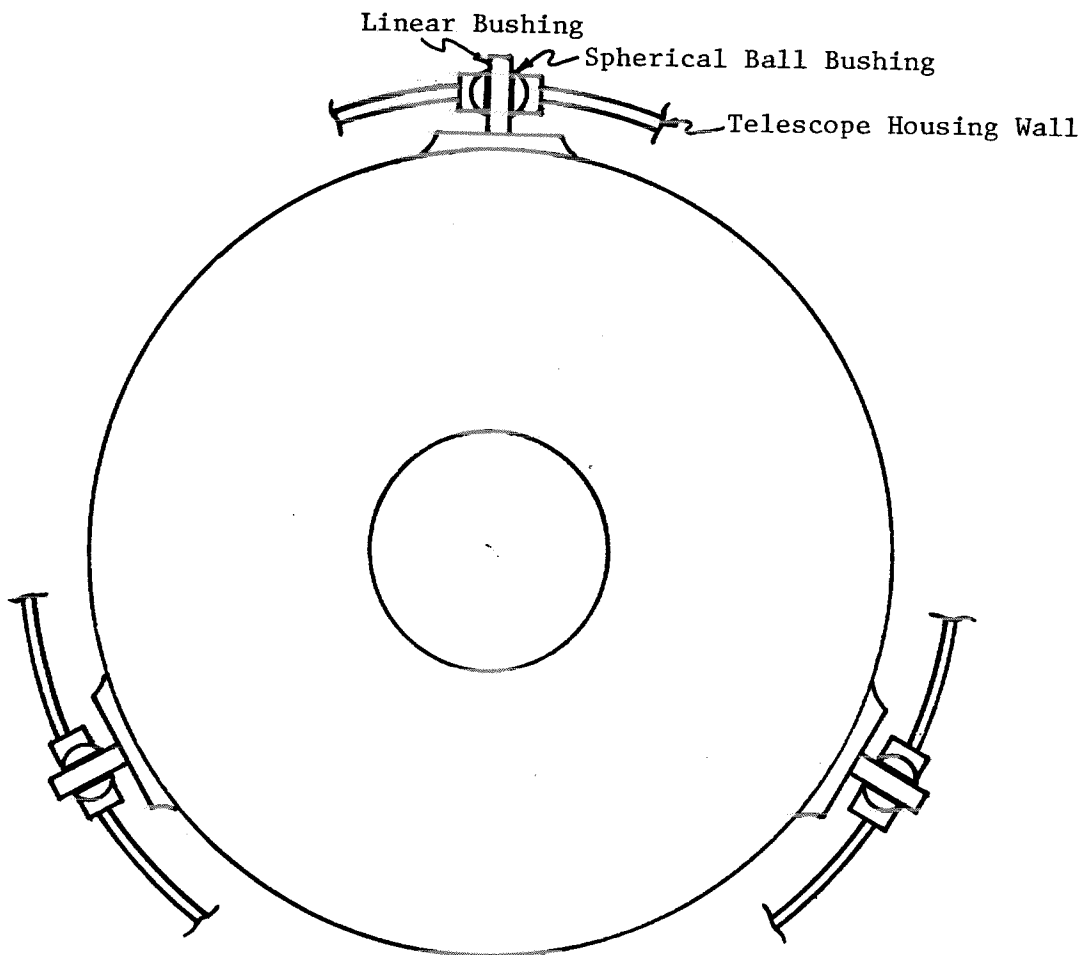


Figure 2. Kinematic Mirror System for ETM Primary Mirror

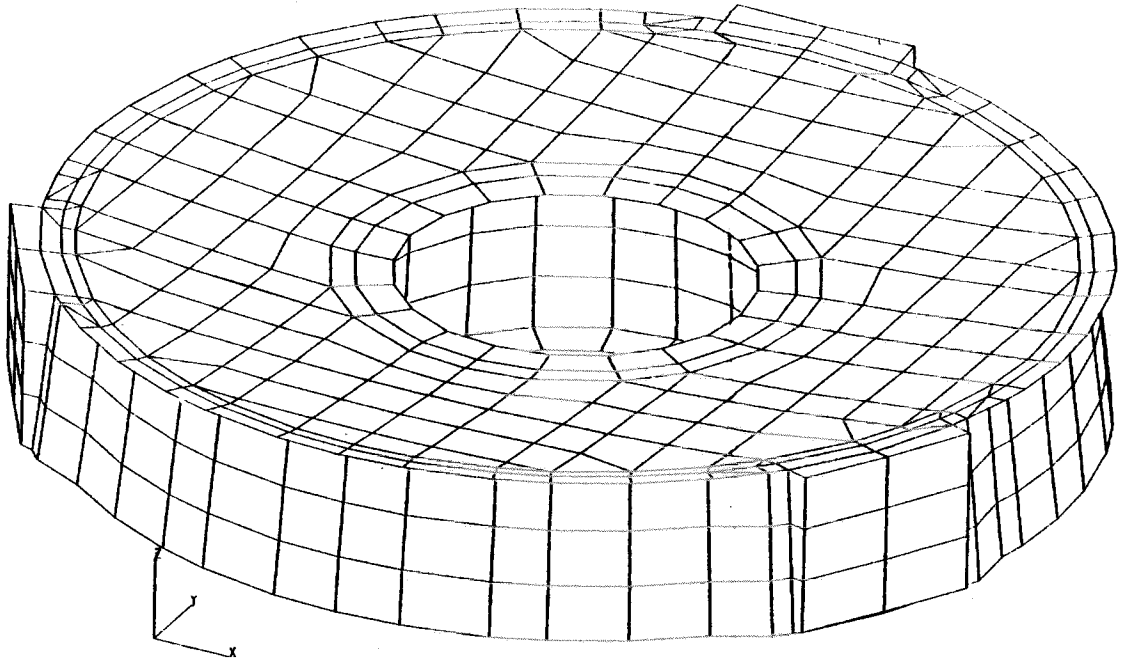


Figure 3. Finite Element Mesh of ETM Primary Mirror

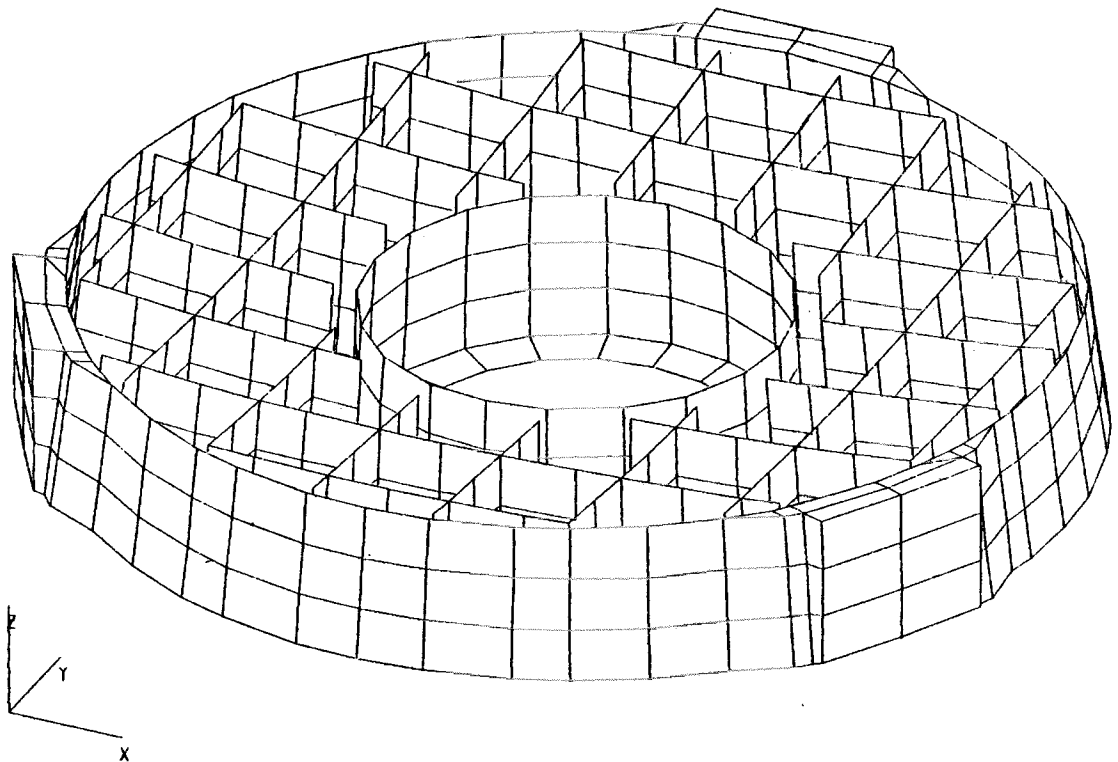


Figure 4. Finite Element Mesh with Mirror Surface Removed

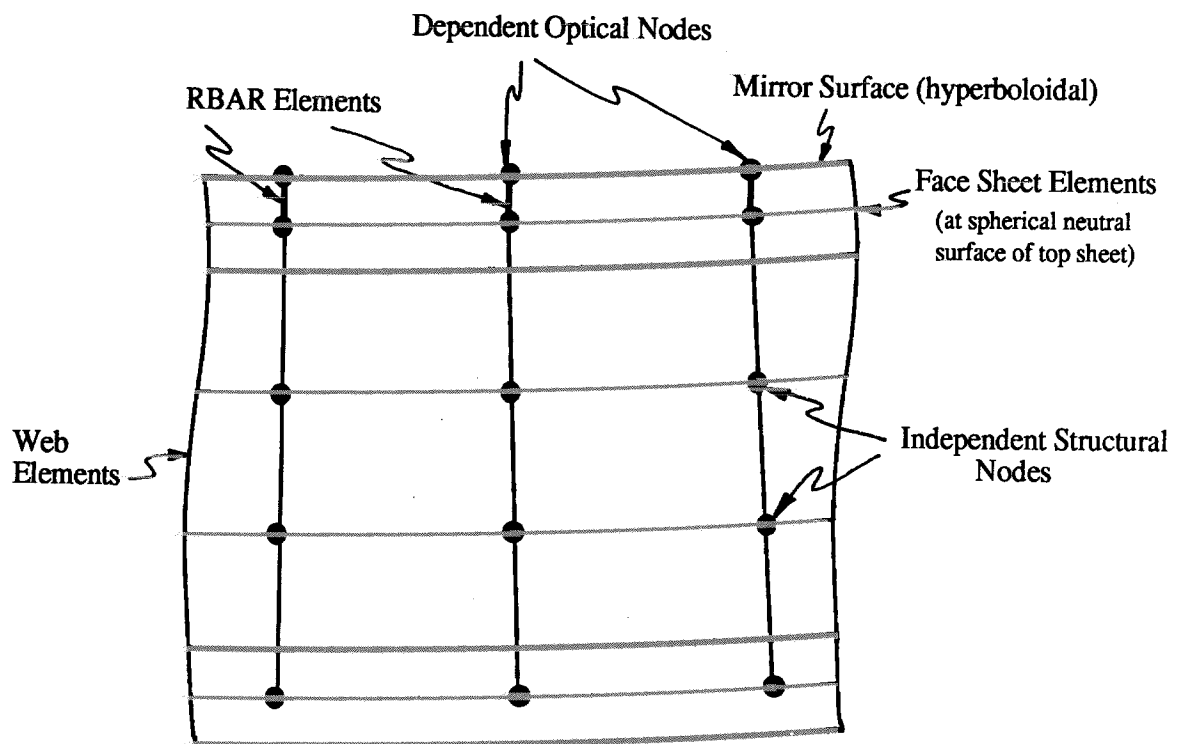
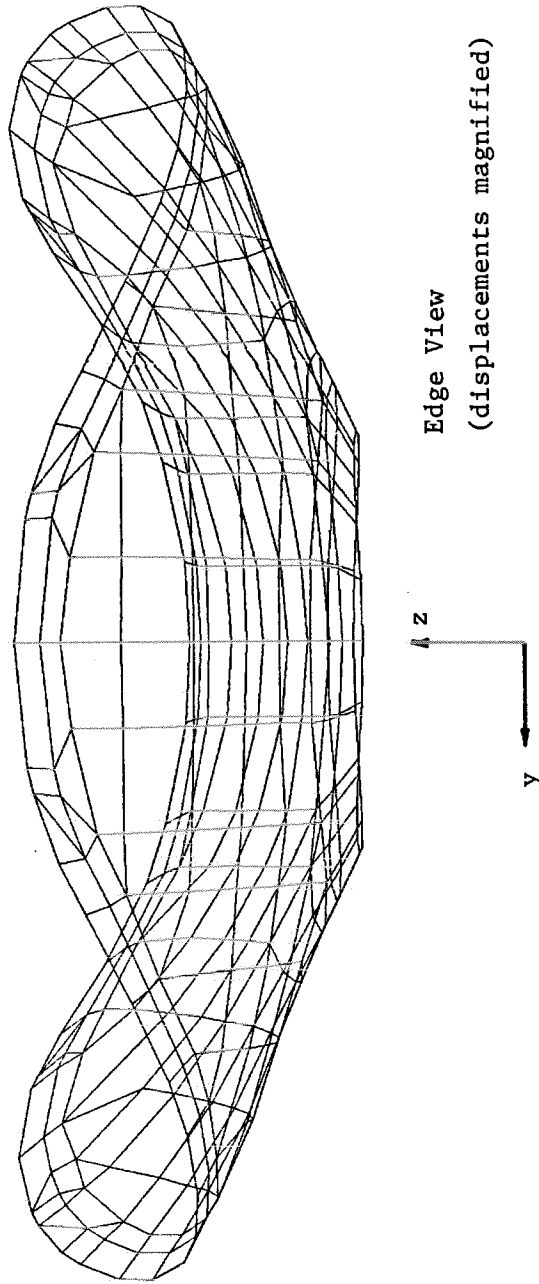


Figure 5. Sectional View of Primary Mirror Finite Element Model



ETM PRI. MIRROR ANALYSIS
 DISPLACEMENT SOLUTION
 1G LOAD IN -Z DIRECTION SUBCASE 1

Figure 6. Deformed Primary Mirror Due to 1-g Load in z-Direction (normal to focal plane).

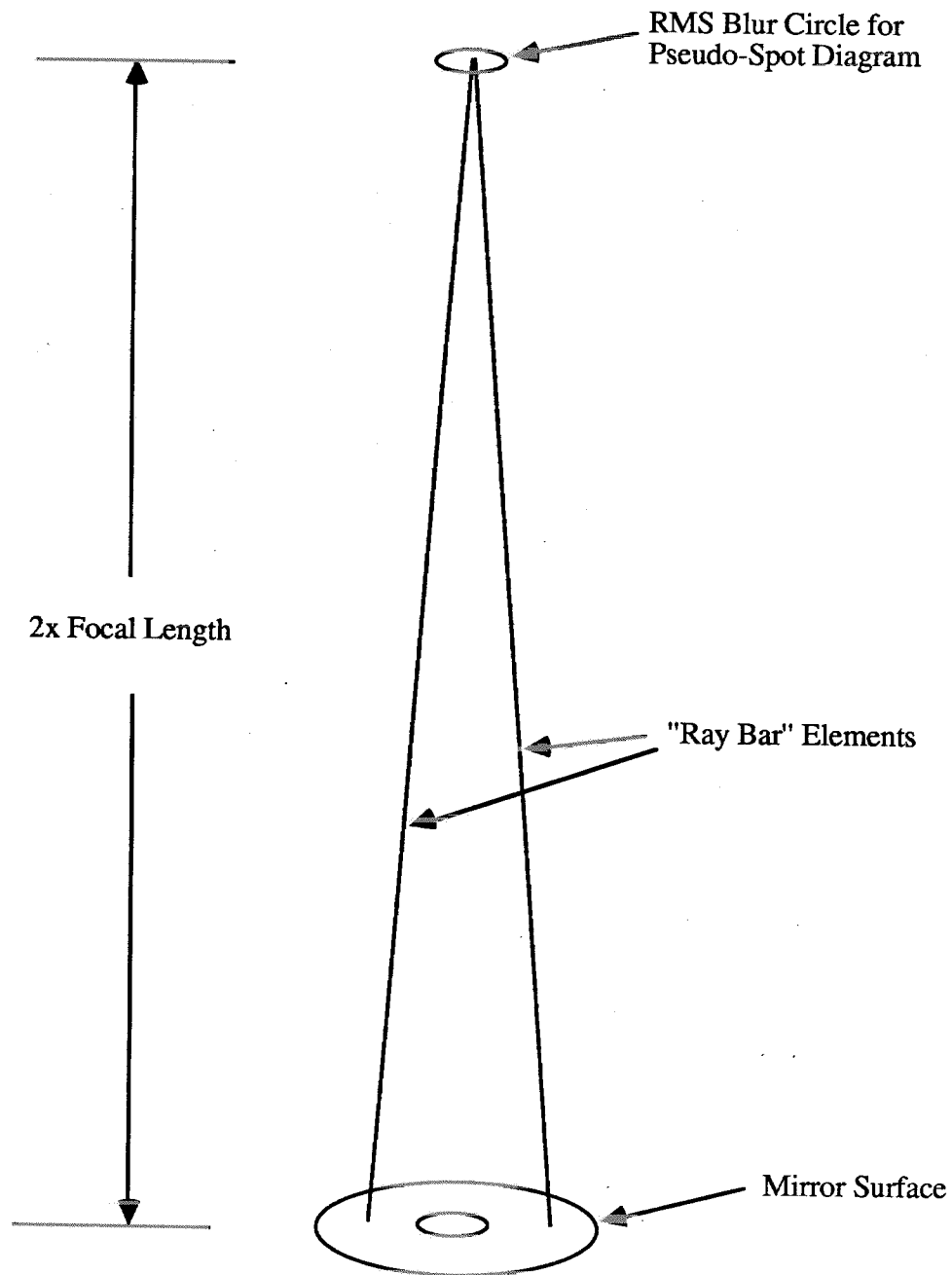


Figure 7. "Ray Bar" Elements from Mirror Surface to Focal Plane

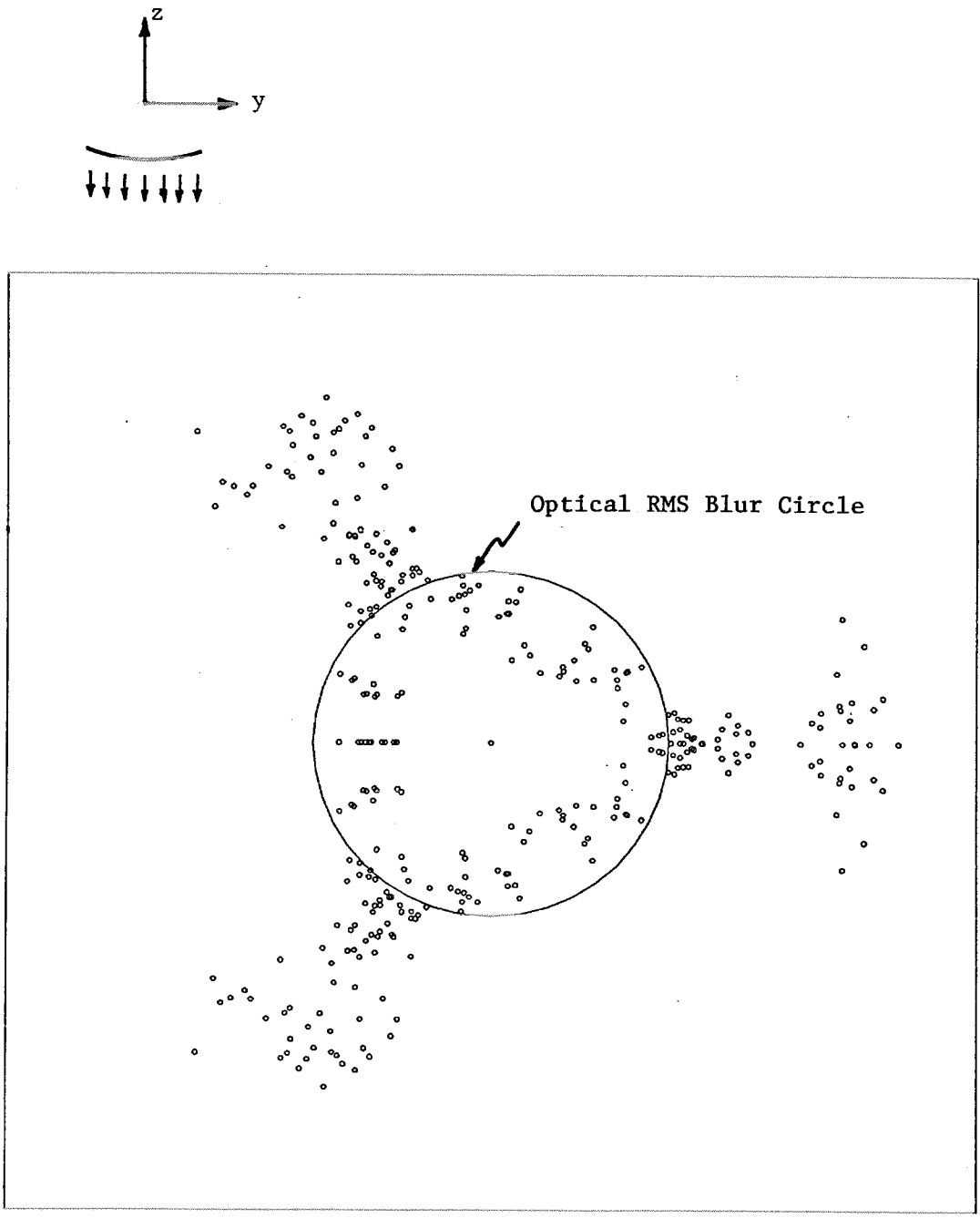


Figure 8. Pseudo-spot Diagram for 1-g Out-of-plane (z-direction) Gravity Load Case.

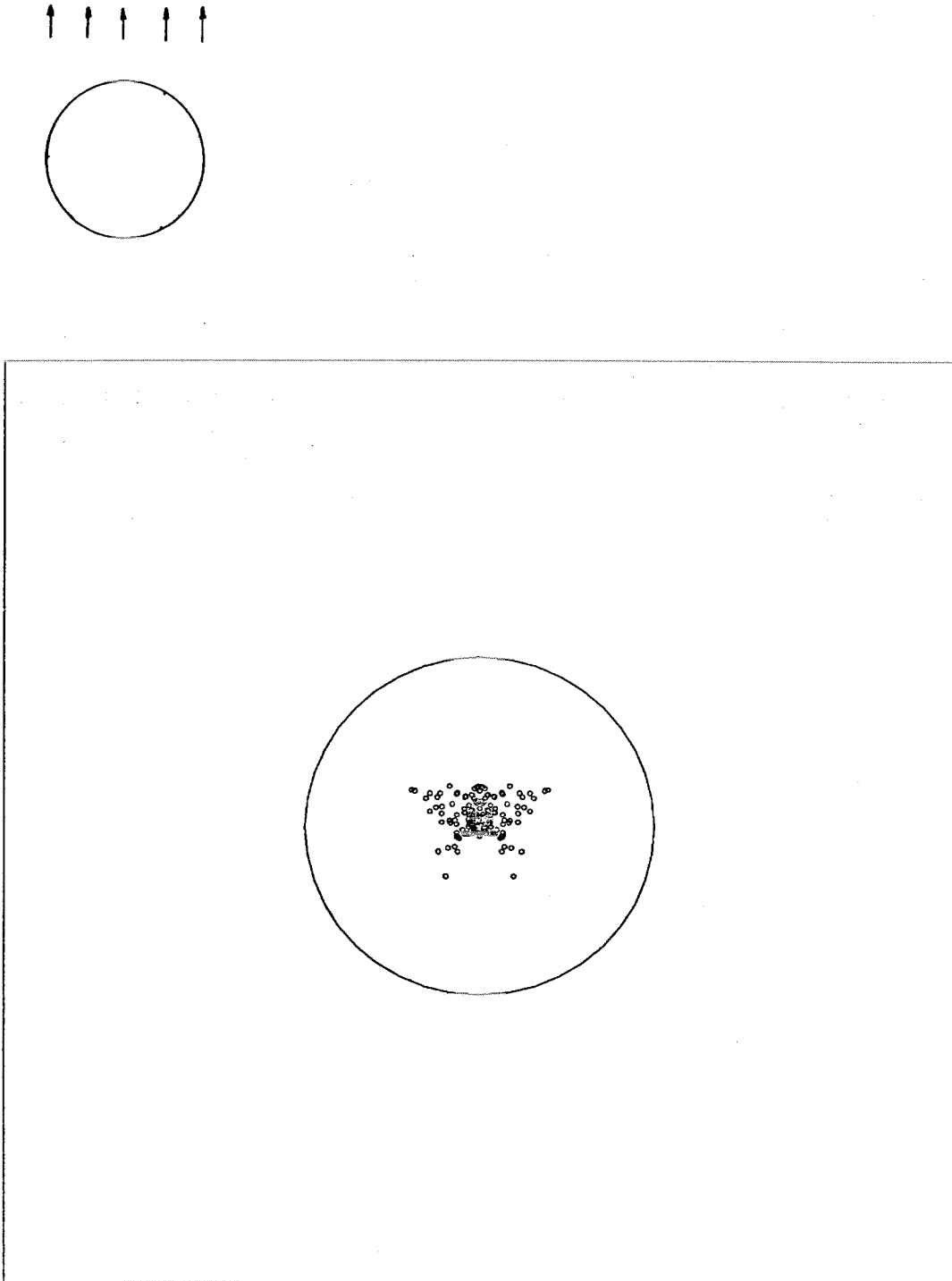


Figure 9. Pseudo-spot Diagram for 1-g
In-Plane (x-direction) Gravity Load Case

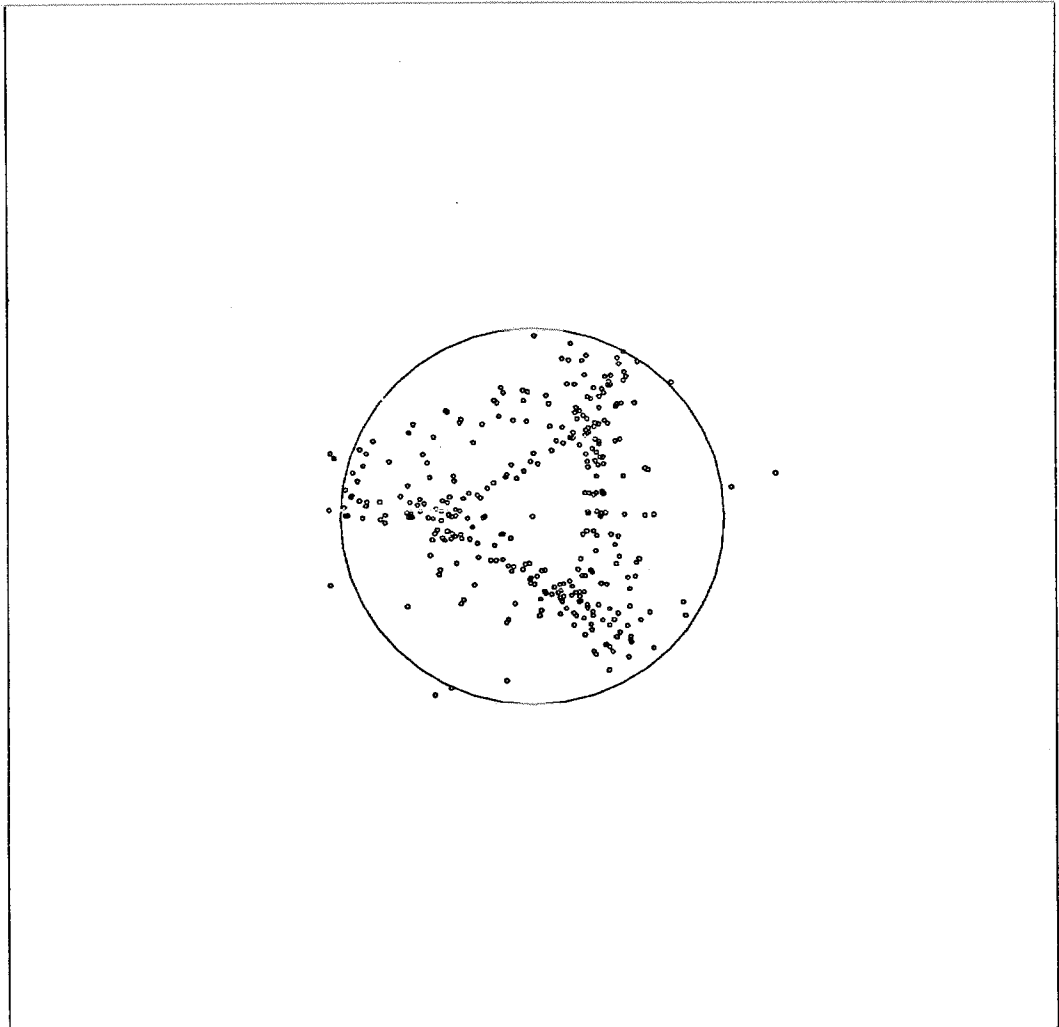
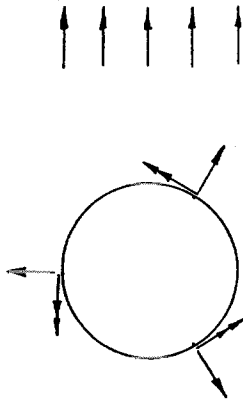


Figure 10. Pseudo-spot Diagram for 1-g In-plane Gravity Loads Combined with Torsional and Radial Bearing Friction Loads.